

# Structure and properties of AA3003 alloy produced by accumulative roll bonding process

Z. P. XING

*Beijing Institute of Aeronautical Materials, Beijing 100095, People's Republic of China;  
Korea Institute of Machinery & Materials, 66 Sangnam-Dong, Changwon, Korea 641-010*

S. B. KANG, H. W. KIM

*Korea Institute of Machinery & Materials, 66 Sangnam-Dong, Changwon, Korea 641-010*

The investigation of the microstructure and mechanical properties has been conducted on AA3003 alloy produced by a novel intense plastic straining process named accumulative roll-bonding (ARB). The results show that ultra-fine grained 3003 alloy having mean grain size of 700–800 nm was successfully produced by the 250°C-ARB. The average grain sizes of 250°C-ARB samples were reduced greatly from about 10.2  $\mu\text{m}$  initially to 700–800 nm. After 6 cycles of ARB, the whole volume of the material was filled with ultra-fine grains with high angle boundaries. The tensile strength of the ARB processed 3003 alloy (after 6 cycles) is considerably higher than that of the initial material, and about 1.5 times higher than that of commercially available fully-hardened (H18) 3003 alloy. Strengthening in ARB processed 3003 alloy may be attributed to strain hardening and grain refinement hardening.

© 2002 Kluwer Academic Publishers

## 1. Introduction

For improving the formability and mechanical properties of the aluminum alloys, one of the best ways is to obtain ultra-fine grains (nanocrystalline and submicron grains). Ultra-fine grains less than 1  $\mu\text{m}$  in diameter can be obtained by intense plastic straining. Several techniques are now available for producing the high strains, including cyclic extrusion compression (CEC) [1], torsion straining under high press (TS) [2], equal channel angular press (ECAP) [3, 4], but one disadvantage of these processes is that they are not applicable to large bulk materials.

One of novel intense straining processes for bulk materials using rolling deformation, named accumulative roll bonding (ARB), was developed recently [5–8]. In this process, the achieved strain is theoretically unlimited. The ARB process has been successfully applied to aluminum 1100 alloy [5, 6], Al-Mg 5083 alloy [7], Al-Fe-Si 8011 alloy [9] and Ti-added interstitial free steel [7, 8]. Most of several cycle ARB processed materials have structures with sub-micron grains and show very high strength at ambient temperature [5–8]. Though having the sub-micro grains by ARB, only 8011 alloy shows a softening behavior after intense straining [9].

The 3003 alloy has more strength than 1100 alloy due to the alloying element Mn. It has been widely used as general purpose alloys for moderate-strength applications requiring good workability [10, 11]. The purpose of the present study is to clarify whether it is possible to produce the 3003 alloy with ultra-fine grains and high strength by ARB process.

## 2. Experimental procedures

The material used in this study was AA3003 alloy whose chemical composition was shown in Table I. Fully annealed 3003 sheets with the initial thickness of 1.0 mm were prepared. The repeated cycle of ARB process can be simplified as follow:

Cutting → Surface treatment → Stacking → Heating → Roll bonding.

Firstly, the initial materials were cut to the sheets with the dimension of 1.0 mm in thickness, 30 mm in width and 300 mm in length. Then the interface between two sheets was degreased by acetone and wire-brushed. After that, the two sheets were layered to make brushed surface in contact and fixed each other closely by wires. They were held in an electrical furnace at 200°C or 250°C for 5 minutes, and then rolled. The sheets were air-cooled after rolling. ARB process was conducted under the conditions that the reduction in thickness per cycle was 50% (equivalent strain of 0.8). The rolling diameter was 175 mm and the roll peripheral speed was about 1 m/min. In order to avoid propagation of edge cracks or center fracture in following cycles, both edges of the roll-bonded sheet were trimmed by shearing and both ends of the sheet were cropped. The rolled sheets (1 mm in thickness) was cut into two pieces with the size similar to the initial material, and then the above procedures were repeated up to 8 cycles.

For examining the effect of the processing condition 200°C/5min or 250°C/5min on the hardness of ARBed 3003 alloy, some of the ARBed samples were annealed again at 200°C (or 250°C) for 5 minutes. The

TABLE I Chemical composition of AA3003 alloy (mass%)

| Elements | Si    | Fe    | Cu    | Mn    | Mg    | Cr    | Zn    | Ti    | Al   |
|----------|-------|-------|-------|-------|-------|-------|-------|-------|------|
| Content  | 0.286 | 0.560 | 0.118 | 1.039 | 0.046 | 0.006 | 0.000 | 0.031 | Bal. |

Vickers microhardness of these samples is equivalent to those samples just taken out of furnace and before roll-bonding.

The values reported for Hv represent the average of seven separate measurements taken at randomly selected points using a load of 200 g for 15 seconds. The tensile specimens were machined from the rolled sheets according to the ASTM E8M standard, oriented along the rolling direction. The gauge length was 25 mm. Tensile tests at room temperature were conducted on a standard universal testing machine at a strain rate of  $8.3 \times 10^{-4} \text{ s}^{-1}$ .

The optical examination of the samples was conducted under conditions of polarized light. Etching was carried out electrolytically using Baker's solution of 5 ml  $\text{HBF}_4$  and 200 ml distilled water and a stainless steel cathode. All optical microstructures were observed along the transverse direction of the rolling samples. The fracture surfaces of the tensile samples were examined by a JSM-5800 scanning electron microscope (SEM).

Specimens were also examined using a JEM-2000 FX II transmission electron microscope (TEM) operating at 200 kV. Thin foils parallel to the rolling plane were prepared by a twin-jet electro-polisher using a solution of 140 ml  $\text{HNO}_3$  and 280 ml  $\text{CH}_3\text{OH}$ . Selected area electron diffraction (SAD) patterns were taken from regions having diameter of  $3 \mu\text{m}$ . Measurements of the grain size were made directly from the optical micrographs (initial materials) and TEM photomicrographs (ARB samples) using an Image & Microscopy Program. At least 100 different grains in every condition were chosen.

### 3. Results

#### 3.1. Effect of processing temperature on mechanical properties

For the  $200^\circ\text{C}$ -ARB samples, some began to crack in the center or in the edge during the 4 cycles, and all the samples began to crack during the 5 cycles. So the rolling temperature  $200^\circ\text{C}$  is too low for 3003 alloy to proceed the ARB process. For the  $250^\circ\text{C}$ -ARB samples, no samples cracked even after 8 cycles.

The Vickers microhardness of 3003 alloy with the number of cycles is presented in Fig. 1. It shows that the Vickers microhardness of  $200^\circ\text{C}$ -ARB samples increased with increasing the cycles up to the 4 cycles. Then the samples began to crack due to the high internal stress. Meanwhile, the Vickers microhardness of the  $250^\circ\text{C}$ -ARB samples increased with increasing the cycles to the 5 cycles and then kept a constant value.

Fig. 2 presents the ambient tensile properties of 3003 alloy. It can be seen that the strength tendency of the samples is nearly the same with their microhardness change. The strength of  $200^\circ\text{C}$ -ARB samples increased

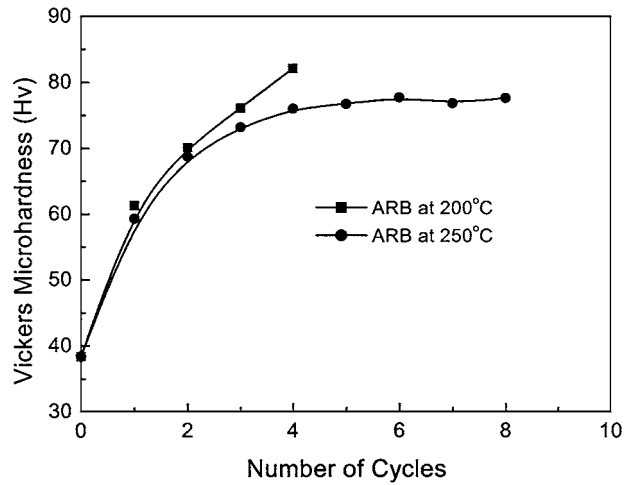


Figure 1 Variation of Vickers microhardness of 3003 alloy with increasing the cycles of ARB at  $200^\circ\text{C}$  and  $250^\circ\text{C}$ .

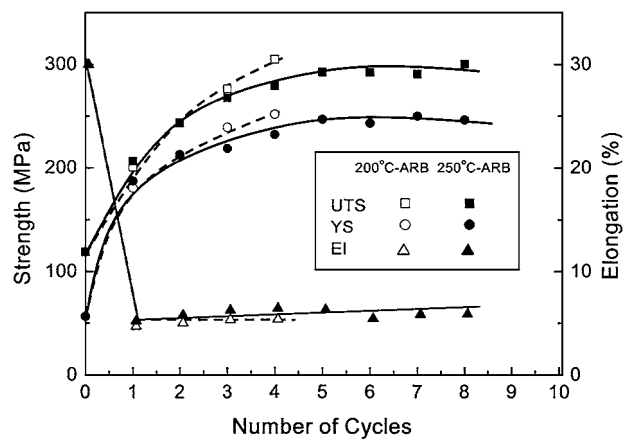


Figure 2 Variation of ambient tensile properties of 3003 alloy with increasing the cycles of ARB at  $200^\circ\text{C}$  and  $250^\circ\text{C}$ .

with the cycles up to 4 cycles and that of  $250^\circ\text{C}$ -ARB samples increased up to 5 cycles. After that, the strength of  $250^\circ\text{C}$ -ARB samples leveled off. Furthermore, their elongation decreased greatly after the first cycle and then it kept a constant value. The tensile strength, yield strength and elongation of commercially available full-hardened 3003 alloy (H18 temper) at room temperature were reported as 200 MPa, 185 MPa and 10%, respectively [10]. So the tensile strength of the ARB processed 3003 alloy (after 6 cycles) is about 1.5 times higher than that of the H18 processed 3003 alloy. Furthermore, mechanical properties and their changing tendency in  $250^\circ\text{C}$ -ARBed 3003 alloy is very similar with those in  $200^\circ\text{C}$ -ARBed 1100 alloy [5, 6].

#### 3.2. Microstructure evolution of ARBed 3003 alloy

Fig. 3 presented the optical micrographs of  $250^\circ\text{C}$ -ARBed samples. The initial specimen showed a typical recrystallized structure with equiaxed grains, and its mean grain size was about  $10.2 \mu\text{m}$  (Fig. 3a). After 1 cycle of ARB (Fig. 3b), sheared grains along the rolling direction were clearly observed. But after 3 cycles, the elongated grains were very thin and were difficult to distinguish by optical microscope (Fig. 3c and d). The

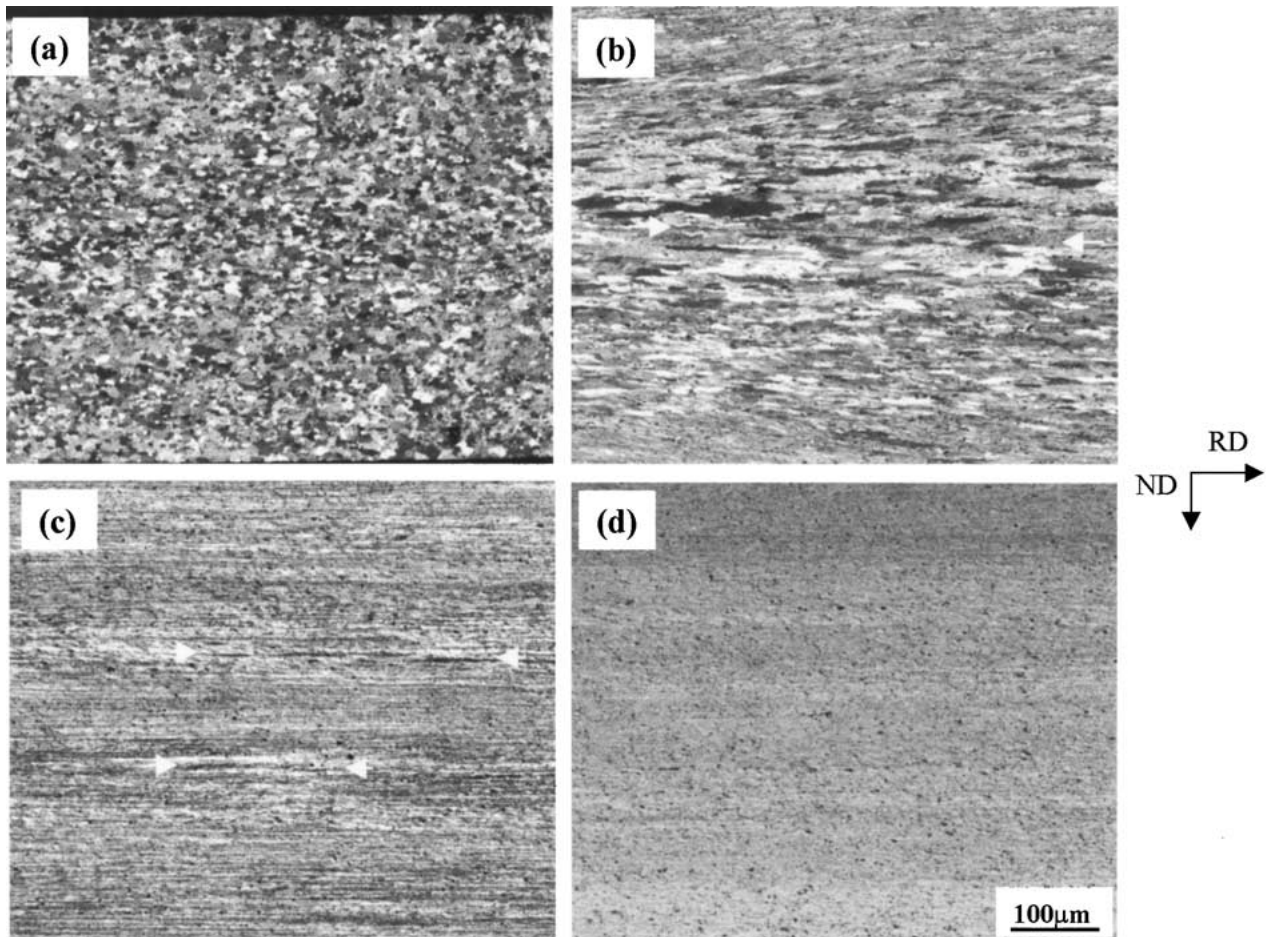


Figure 3 Optical microstructures of 3003 alloy after 250°C-ARB. (a) 0 cycle, (b) 1 cycle (strain of 0.8), (c) 3 cycles (strain of 2.4), and (d) 6 cycles (strain of 4.8).

interfaces (indicated by the arrows in Fig. 3b and c) introduced in every cycle were partly observed only by chemical etching. This indicates the bonding of the interfaces was quite good.

For further observing the bonding condition, the fracture surfaces after tensile test were observed by SEM (Fig. 4). It shows that the initial material exhibited a typical ductile fracture showing dimples and outside shear zones (Fig. 4a). Great deformation and necking can be seen in macro level. After ARB process, the samples also show a ductile fracture having the dimples and shear zones. But a little deformation and small necking happened. The dimples were not so deep as those in initial material (Fig. 4b–d). Except outside shear zones, there also existed shear zones between the interfaces formed in the last pass. The interfaces formed in the 1 cycle and 3 cycles samples were indicated in Fig. 4b and c, respectively. There were total 255 ( $2^8 - 1$ ) interfaces in the 8 cycles sample so that the thickness of the initial sheets after 8 cycles was reduced to  $1/2^8$  mm ( $\sim 3.9 \mu\text{m}$ ). So it is difficult to indicate the individual interface in Fig. 4d. Only the interface formed in the last pass was given in the Figure. From Fig. 4b–d, it can be seen that debonding happened in the interface formed in the last pass (reduction 50%). However, debonding did not happen obviously in the interfaces formed in the other passes (reduction  $\geq 75\%$ ). So the interface formed in the last pass (reduction of 50%) was not strong enough. Only after deformation more than 75%

reduction, the interfaces could bond very well. Therefore, after the final ARB pass, the materials should further be rolled with reduction at least 50%. In that case, all the interfaces (reduction  $\geq 75\%$ ) are supposed to be bonded very well, and the ductility may be improved for some extent.

Fig. 5 shows TEM microstructures and corresponding SAD patterns of the base alloy after various cycles of 250°C-ARBed samples. After 1 cycle (Fig. 5a), the SAD pattern shows the net pattern indicative of low angle boundaries. So the grain structure at this stage was consisted of subgrains. The grain structure of the 2 cycles sample was nearly the same with that of 1 cycle sample except the increased misorientation angles of the boundaries for some extent (Fig. 5b). After 3 cycles, most of the SAD patterns also show single net patterns. This means most of the specimen still had subgrain structure at this stage. But some regions show scattered diffraction patterns which show the existence of ultra-fine grain with high angle boundaries. The fraction of the ultra-fine grains increased with the cycles up to 6 cycles. After 6 cycles (Fig. 5d), all the SAD patterns show the presence of high angle grain boundaries due to the distribution of diffraction spots around circles. This means the whole volumn of the material was filled with ultra-fine grains. The average grain sizes (sub-grain sizes in 1–3 cycle samples) of the ARB processed 3003 alloy with the number of the ARB cycles are presented in Fig. 6. The average grain (or subgrain) sizes of

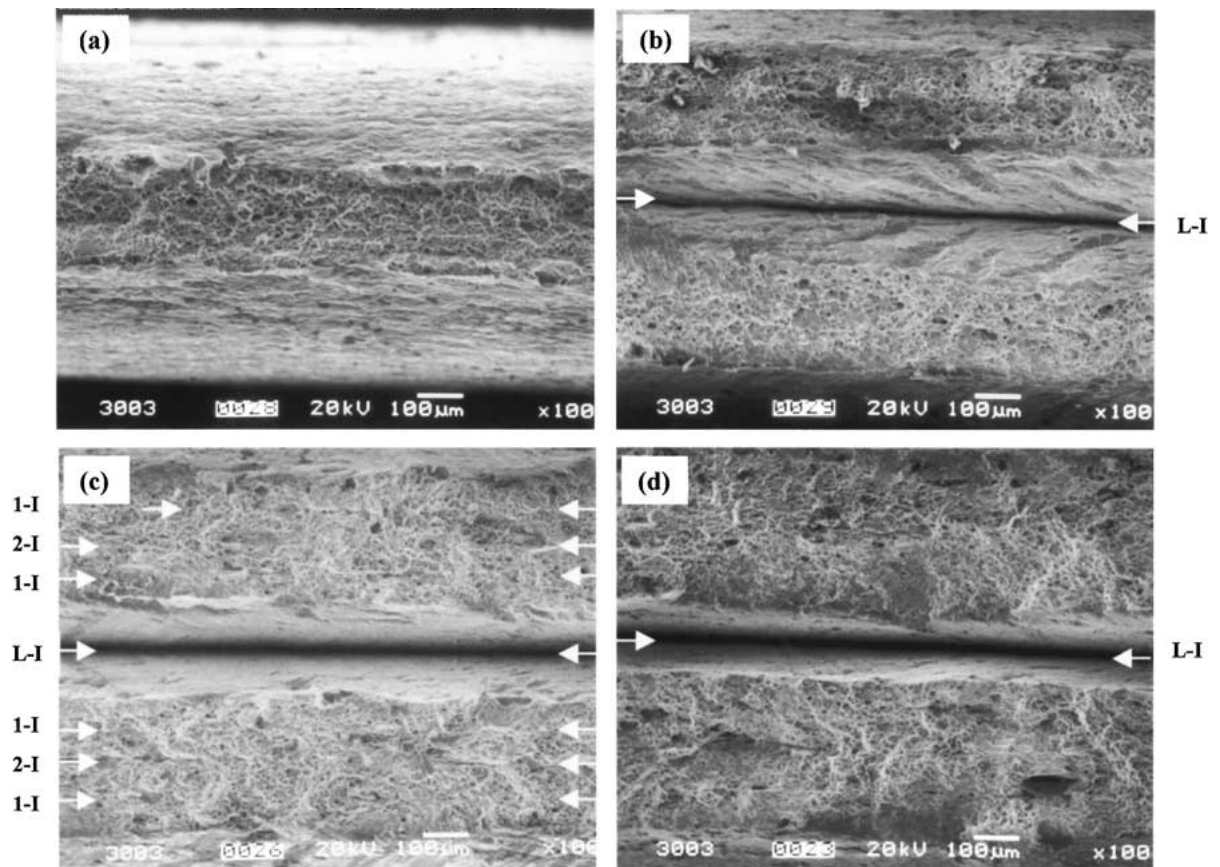


Figure 4 Tensile fracture surfaces of 3003 alloy after 250°C-ARB. (a) 0 cycle, (b) 1 cycle, (c) 3 cycles, and (d) 8 cycles. L-I: Interface formed in the last pass, 1-I: Interface formed in the first pass, and 2-I: Interface formed in the second pass.

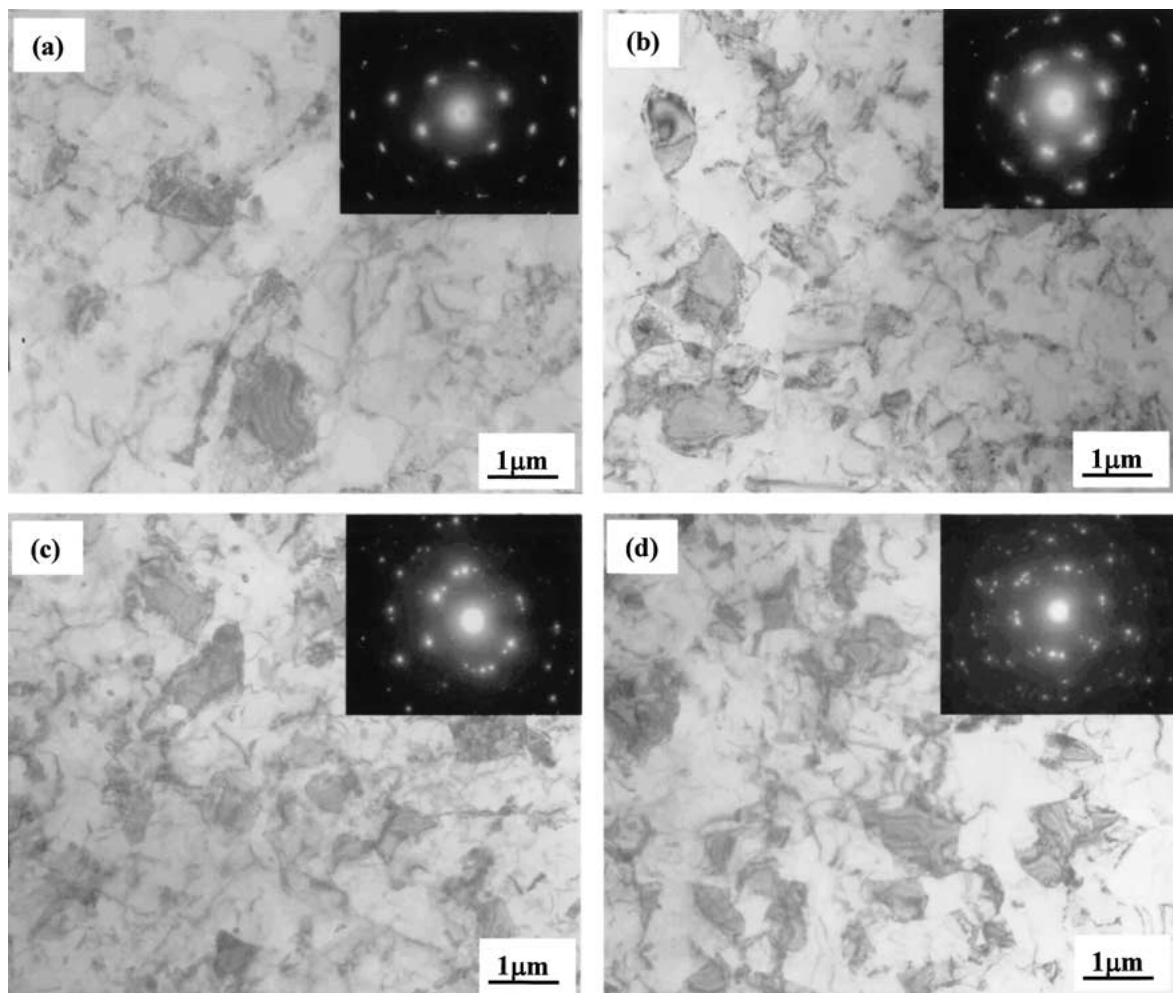


Figure 5 TEM micrographs and corresponding SAD patterns of 3003 alloy after 250°C-ARB. (a) 1 cycle, (b) 2 cycle, (c) 3 cycles, and (d) 6 cycles.

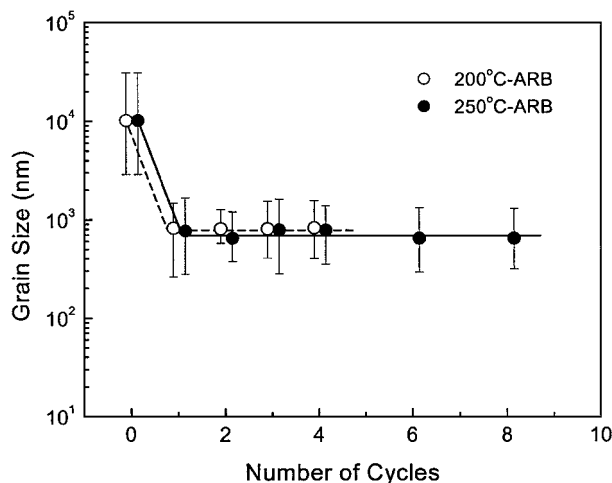


Figure 6 Variation of grain sizes of 3003 alloy with increasing the cycles of ARB.

250°C-ARB samples were reduced greatly from about 10.2  $\mu\text{m}$  initially to about 770 nm after 1 cycle of ARB. Then they changed slightly in the range of 700–800 nm during 1–8 cycles of ARB. Interestingly, the grain (or subgrain) sizes of 200°C-ARB samples were nearly the same with those of 250°C-ARB samples, and their values were in the range of 750–800 nm during 1–4 cycles of ARB (Fig. 6). However, the grain (or subgrain) sizes formed in 3003 alloy was slightly bigger than those (670 nm) in 1100 alloy made by 200°C-ARB [5, 6].

#### 4. Discussion

Accumulative Roll-Bonding (ARB) process is an excellent and new processing technique for establishing ultra-fine (sub-micrometer) grains in metallic alloys. The advantage of this process against other high straining process is its high productivity and the feasibility of large-sized material production [7]. A higher strength was obtained in some aluminum alloys such as 1100 alloy [5, 6], 5083 alloy [7] and 3003 alloy in this study.

Different processing temperature of ARB should be chosen in consideration of physical properties of alloys. If the temperature is too high, the softening behavior may happen [9]. On the other hand, if the temperature is not high enough, not only the interface bonding is very weak, but also edge cracks or center fracture may take place. The processing condition of 200°C/5min is suitable for the ARB process of 1100 alloy and 5083 alloy [5–7], but the temperature is too high for the 8011 alloy [9] and quite lower for the 3003 alloy. Fig. 7 presents the effect of the annealing condition 200°C/5min or 250°C/5min on the hardness of ARB processed 3003 alloy. It can be seen that the 200°C/5min annealing had nearly no effect on the hardness of 200°C-ARB samples (Fig. 7a). Therefore, in 200°C-ARB process, the applied strain energy was continually accumulated until samples happened to crack during and after 4 cycles. Meanwhile, the 250°C/5min annealing decreased the hardness of ARB samples during every cycles (Fig. 7b). The decreasing extent increased with increasing the cycles up to 4 cycles. After that, the decreasing extent kept nearly no change. The average grain (or subgrain)

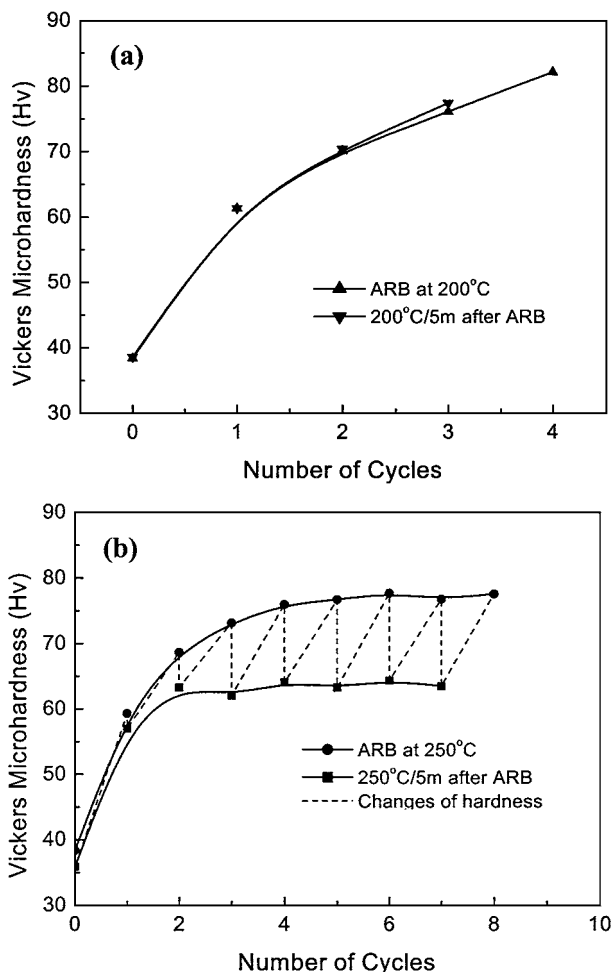


Figure 7 Effect of the annealing condition 200°C/5min or 250°C/5min on the hardness of ARB processed 3003 alloy. (a) 200°C-ARB, and (b) 250°C-ARB.

size of 200°C-ARB samples after 200°C/5min annealing was about 760 nm, nearly the same with that of as-ARB samples. However, the average grain (or subgrain) size of 250°C-ARB samples after 250°C/5min annealing was about 900 nm, slightly bigger than that of as-ARB samples. In order to proceed ARB process continually, the static recovery which results in grains (or subgrains) growing should take place in some extent during annealing period. For 3003 alloy, the annealing condition 250°C/5min is suitable for the ARB process.

The strengthening in 250°C-ARB processed 3003 alloy may be attributed to strain hardening and grain refinement hardening, which is the same with that in 1100 alloy [5]. Up to 2 cycles, strain hardening may play a main role in the strength increase, and the formation of submicrometer subgrains also contribute to the strength for some extent. From 3 cycles, the strength increase is most probably due to the evolution of the grain structure. Strain hardening has less and less effect on it. Because the number of ultra-fine grains with high angle grain boundaries increase with increasing the cycles up to 6 cycles. This tendency is the same with those of strength and hardness. Furthermore, the ductility decrease is mainly influenced by the strain hardening. However, debonding in the interfaces formed in the last pass also plays an important role in the ductility decrease.

For improving the interface bonding strength, we suggest that the ARB processed 3003 alloy should further be rolled with reduction 50% at least after the final pass of ARB, and make all the interfaces experienced reduction more than 75% (equivalent strain of 1.6).

## 5. Conclusions

(1) Ultra-fine grained 3003 alloy having mean grain size of 700–800 nm was successfully produced by the ARB process. The annealing condition 250°C/5min is suitable for the ARB process.

(2) The number of the grains with high angle grain boundaries increased with increasing the cycles up to 6 cycles. After 6 cycles, the whole volume of the material was filled with fine grains with high angle grain boundaries.

(3) The strength of 250°C-ARB samples increased with increasing the cycles up to 5 cycles and then kept a constant value. And their elongation decreased greatly after the first cycle and then it kept nearly no change. The tensile strength of the ARB processed 3003 alloy (after 6 cycles) is about 1.5 times higher than that of commercially available fully-hardened (H18) 3003 alloy.

(4) The strengthening in ARB processed 3003 alloy may be attributed to strain hardening and grain refinement hardening.

(5) For improving the interface bonding strength, we suggest that the ARB processed 3003 alloy should further be rolled with reduction 50% at least after the final pass of ARB.

## References

1. J. RICHERT and M. RICHERT, *Aluminium* **62** (1986) 604.
2. R. Z. VALIEV, R. R. MULYUKOV, V. V. OVCHINNIKOV and V. A. SHABASHOV, *Scr. Mater.* **25** (1991) 2717.
3. R. Z. VALIEV, N. A. KRASILNIKOV and N. K. TSENEV, *Mater. Sci. Eng. A* **137** (1991) 35.
4. Y. IWAHASHI, Z. HORITA, M. NEMOTO and T. G. LANGDON, *Acta Mater.* **45** (1997) 4733.
5. Y. SAITO, N. TSUJI, H. UTSUNOMIYA, T. SAKAI and R. G. HONG, *Scr. Mater.* **39** (1998) 1221.
6. Y. SAITO, H. UTSUNOMIYA, N. TSUJI, T. SAKAI and R. G. HONG, *J. Japan Inst. Metals.* **63** (1999) 790.
7. Y. SAITO, H. UTSUNOMIYA, N. TSUJI and T. SAKAI, *Acta Mater.* **47** (1999) 579.
8. N. TSUJI, Y. SAITO, H. UTSUNOMIYA and S. TANIGAWA, *Scr. Mater.* **40** (1999) 795.
9. Z. P. XING, S. B. KANG and H. W. KIM, *ibid.* **45** (2001) 597.
10. J. R. DAVIS, "ASM Specialty Handbook: Aluminium and Aluminium Alloys" (Materials Park, Ohio: ASM International, 1993) p. 59, p. 669.
11. P. A. HOLLINSHEAD and T. SHEPPARD, *Mater. Sci. Tech.* **3** (1987) 1019.

*Received 20 March*

*and accepted 2 October 2001*